Processing and Application of Ceramics 15 [1] (2021) 32–39
https://doi.org/10.2298/PAC2101032A



# The interaction between cerium dioxide, lanthanum and europium oxides at 1500 °C

Olena R. Andrievskaya[1], Oksana A. Kornienko[1,*], Oleksandr I. Bykov[1], Olga V. Chudinovich[1], Larysa N. Spasonova[2]

[1]*Frantsevich Institute for Materials Science Problems NAS, Kiev - Ukraine, 3 Krzhizhanovsky str., Kyiv, 03680, Ukraine*
[2]*National Technical University of Ukraine "Igor Sikorsky Kyiv Polytechnic Institute", 37 Victory Ave., Kyiv, 03056, Ukraine*

Received 2 April 2020; Received in revised form 5 August 2020; Received in revised form 30 October 2020; Accepted 30 December 2020

## Abstract

*Materials based on $CeO_2$-$La_2O_3$-$Eu_2O_3$ and $La_2O_3$-$Eu_2O_3$ systems are promising candidates for a wide range of applications, but the phase relationship has not been studied systematically previously. The phase relations in the $CeO_2$-$La_2O_3$-$Eu_2O_3$ ternary system at 1500 °C and binary $La_2O_3$-$Eu_2O_3$ system at 1600–1500 °C were studied in air by X-ray diffraction (XRD) investigation in the overall concentration range. The isothermal section of the phase diagram for the $CeO_2$-$La_2O_3$-$Eu_2O_3$ system has been constructed. It was established that in the ternary $CeO_2$-$La_2O_3$-$Eu_2O_3$ system there exist fields of solid solutions based on hexagonal (A) modification of $La_2O_3$, cubic modification of $CeO_2$ with fluorite-type structure (F), cubic (C) and monoclinic (B) modification $Eu_2O_3$. It was established that in the binary $La_2O_3$-$Eu_2O_3$ system there exist fields of solid solutions based on hexagonal (A) modification of $La_2O_3$ and monoclinic (B) modification $Eu_2O_3$. The phases were separated by two-phase fields (A+B). The refined lattice parameters of the unit cells for solid solutions and microstructures of the definite field of compositions for the systems were determined.*

***Keywords:*** *$CeO_2$, phase diagrams, X-ray diffraction (XRD), solid solutions*

## I. Introduction

Stabilization of the particular phase of a solid solution possessing optimal thermal, mechanical, or electrical properties is a challenge relevant to a wide variety of materials ranging from ion conductors to ferroelectrics [1]. The $CeO_2$-$Ln_2O_3$ solid solutions are the subject of numerous structural studies motivated by the fact that Ln-doped ceria is one of the most important oxygen ion conductors for solid oxide fuel cells (SOFC). Structural modification of ceria-based solutions by co-doping is one possible way to increase the ionic oxide conductivity of ceria-based electrolytes at an intermediate temperature range (500–700 °C) [1–10]. Materials co-stabilized with $Gd_2O_3$ or $Eu_2O_3$ and other trivalent cations such as $La^{3+}$, $Nd^{3+}$, $Y^{3+}$, $Bi^{3+}$ or divalent cations $Ca^{2+}$, $Mg^{2+}$, $Sr^{2+}$, depending on chemical composition, have generally improved ionic conductivities, although in some cases a deterioration in ionic conductivity or increased electronic conductivity have been observed [6]. The incorporation of co-doped ceria electrolytes into IT-SOFC produced higher power and current densities from this cell compared with the same SOFC utilised with an oxide membrane single-doped ceria $Ce_{1-x}M_xO_1 \cdot 9$ (M = Gd, Sm, Y and $0.1 < x < 0.3$) [6]. The right choice of an optimal electrolyte depends on the reliability of data on solubility limits for REE oxides in the crystalline lattice of $CeO_2$, since high ion conductivity corresponds to maximal concentration of compensating oxygen vacancies. This, in turn, requires good knowledge of the phase equilibria in multicomponent oxide systems. Investigations of peculiarities of REE polymorphism, exsolution and formation of ordered phases as well as of the effect of electronic structure and relations between ion radii of lanthanides

*Corresponding author: tel: +38 68 1501979,
e-mail: *kornienkooksana@ukr.net*

on the phase transformation, structure, and stability are also of keen scientific interest [10].

The phase relations at the boundary of binary $CeO_2$-$Ln_2O_3$, $La_2O_3$-$Ln_2O_3$ systems have been studied [5,6,10–27]. Phase equilibrium in the binary $CeO_2$-$Ln_2O_3$ systems studied in the past were characterized by the formation of limited solid solutions based on different polymorphs of initial components [5,6,10–27]. The phase equilibria in the $CeO_2$-$Eu_2O_3$ system at 600, 1100 and 1500 °C were studied in the whole concentration range [17–20]. The X-ray analysis showed that three solid solutions of substitution type exist in the $CeO_2$-$Eu_2O_3$ system in the given temperature interval. Two of them have cubic symmetry (fluorite F-$CeO_2$ type and C-$Eu_2O_3$ type) and the third one has monoclinic symmetry (B-$Eu_2O_3$ type). The phases were separated by two-phase fields (C + F; B + C). The number of phase fields decreases with the temperature decrease to 600 °C, because the monoclinic B-$Eu_2O_3$ exists only above 1000 °C [20]. The boundaries of the homogeneity fields at 1500 °C for F-$CeO_2$, C-$Eu_2O_3$ and B-$Eu_2O_3$ solid solutions were determined from the samples containing 20–25 mol%, 80–85 mol% and 95–99 mol% of $Eu_2O_3$, respectively. Similarly, to determine boundaries of the homogeneity fields for F-$CeO_2$ and C-$Eu_2O_3$ solid solutions, samples containing 20–25 mol% and 90–99 mol% of $Eu_2O_3$, respectively, were used for heat treatment at 1100 °C. By reducing the temperature to 600 °C, the homogeneity field of solid solutions based on the F-$CeO_2$ and C-$Eu_2O_3$ were significantly narrowed. The boundaries of this field were defined by the samples containing 10–15 mol% and 97–98 mol% of $Eu_2O_3$, respectively [20].

The solubility of $CeO_2$ in hexagonal A-lanthanum oxide attain 25 mol% at 1500 °C. The A-$La_2O_3$ solid solutions of $CeO_2$-$La_2O_3$ remain stable at 1500 °C. In contrary, $La_2O_3$ on the surface is exposed to water-containing environment and forms lanthanum hydroxide instead of hexagonal phase of $La_2O_3$ for the samples containing from 100 to 70 mol% $La_2O_3$. Increasing of ceria content coincides with the appearance of A-modification of $La_2O_3$, as determined by X-ray diffraction (XRD) patterns [23,24].

Albeit its great prospects for technological applications [1–5], the phase relationship of the ternary $CeO_2$-$La_2O_3$-$Eu_2O_3$ and binary $La_2O_3$-$Eu_2O_3$ systems has not been investigated. In this paper, we present the phase equilibrium in the $CeO_2$-$La_2O_3$-$Eu_2O_3$ ternary and $La_2O_3$-$Eu_2O_3$ binary systems in the whole range of compositions at temperature 1500 °C.

## II. Experimental

The starting materials were $La_2O_3$ of LaO-1 grade, $Eu_2O_3$ (content of the main components reaches 99.99%) and cerium nitrate $Ce(NO_3)_3 \cdot 6H_2O$ of grade "ch" (above 98%). Before being weighed, the oxides were dried in a muffle chamber at 1200 °C (2 h). The samples were prepared with a concentration step of 1–5 mol%. Weighed oxide portions were dissolved in $HNO_3$ (1:1). $Ce(NO_3)_3 \cdot 6H_2O$ was added into a mixture after the oxides were completely dissolved. A homogeneous solution of nitrates was evaporated to remove nitric acid and calcined at 800 °C for 2 h. The powders were subjected to single-action pressing in a steel die without a binder at 10–30 MPa to make pellets 5 mm in diameter and 4 mm in height. Annealing at 1500 °C was conducted via two stages: first in a furnace with H23U5T (fecral) heaters at 1250 °C for 600 h, then in a furnace with molybdenum disilicide heaters at 1500 °C for 80 h in air. The two-step annealing allows removing residuals of nitrogen oxides from the samples. At lower temperatures, ≤1250 °C, phase equilibriums (which include processes of exsolution and ordering) were reached rather slowly because of low velocity of diffusion processes in the cation sublattice, which requires long-term annealing of samples [28]. The synthesis completeness was regularly controlled. Then the samples were pressed and annealed again. Upon annealing for 80 h (1500 °C) no change in the phase composition of the samples was observed. Cooling was conducted inside the furnace. The chemical analysis of the powders was done prior to heat treatment and after it selectively. No changes of the chemical composition were revealed. The prepared samples with different compositions have following notation C*x*-L*y*-E*z*, where *x*, *y* and *z* denote mol% of $CeO_2$, $La_2O_3$ and $Eu_2O_3$, respectively.

XRD analysis of the samples was performed by powder procedure on a DRON-3 apparatus at ambient temperature under $CuK_\alpha$ radiation. Scanning step was 0.05–0.1°, exposition 4 s and $2\theta$ angle interval 10 to 90°. Lattice parameters were calculated by the least square method using the LATTIC program with an error of not lower than 0.0001 nm for the cubic phase. Phase com-

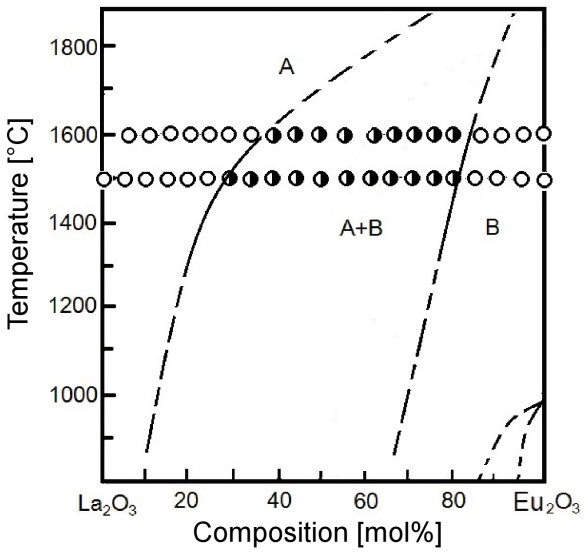


**Figure 1. Phase equilibria in the $La_2O_3$-$Eu_2O_3$ system at 1600–1500 °C (○ - single-phase samples, ◑ - two-phase samples)**

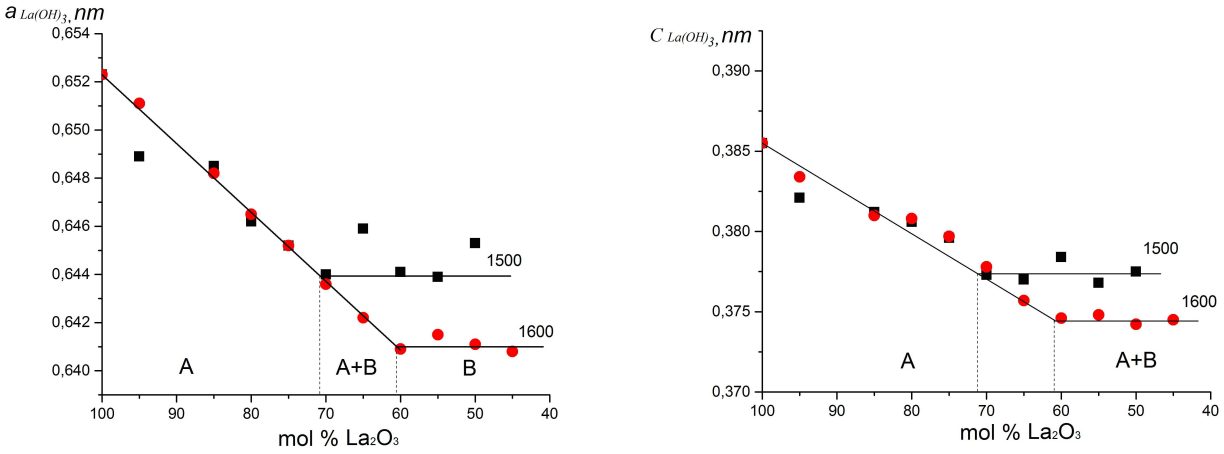


**Figure 2. Concentration dependences of the lattice parameters *a* (a) and *c* (b) of $La(OH)_3$ based solid solutions in the $La_2O_3$-system upon annealing at 1500 and 1600 °C**

position was identified using the base of JSPDS (International Center for Diffraction Data 1999).

## III. Results and discussion

### *3.1. Phase relation in $La_2O_3$-$Eu_2O_3$ system*

The study of solid phase interaction of $La_2O_3$ (hexagonal modification of rare-earth oxide, type A, space group $P63/m$) with $Eu_2O_3$ (monoclinic modification of rare-earth oxide, type B, space group $C2/m$) in the temperature range of 1600–1500 °C revealed that in the $La_2O_3$-$Eu_2O_3$ system two types of solid solutions are formed which have a hexagonal A-$La_2O_3$ and monoclinic B-$Eu_2O_3$ structure. The phases were separated by two-phase fields (A+B) as shown in Fig. 1. It is important to underline that in accordance with the XRD phase analysis, in the samples containing from 20 to 100 mol% of $La_2O_3$, instead of the hexagonal modification of A-$La_2O_3$, the hexagonal lanthanum hydroxide A-$La(OH)_3$ was observed because the samples absorb water from wet air and transform into hydroxide after annealing and cooling. The input chemical and phase compositions of the samples, annealed at 1600 and 1500 °C, and the lattice parameters of the corresponding equilibrium phases at given temperatures are presented in the Supporting Information (Tables 1 and 2). The change in the lattice parameters in A-$La(OH)_3$ and B-$Eu_2O_3$ based solid solutions against the $Eu_2O_3$ concentration is shown in Figs. 2 and 3.

The solubility of $Eu_2O_3$ in A-$La_2O_3$ is 28 mol% at 1500 °C and 38 mol% at 1600 °C (Fig. 1). Data given in Fig. 2 reveal that the lattice parameters decrease from $a$ = 0.6523 nm, $c$ = 0.3855 nm for the pure $La(OH)_3$ to $a$ = 0.6440 nm, $c$ = 0.3773 nm for the two-phase (A+B) sample L70-E30 at 1500 °C and to $a$ = 0.6409 nm, $c$ = 0.3746 nm for the two-phase (A+B) sample L60-E40 at 1600 °C.

The solubility of $La_2O_3$ in the monoclinic B-$Eu_2O_3$ modification is ~19 mol% at 1500 °C and 16 mol% at 1600 °C (Fig. 1). The lattice parameters (Fig. 3) of B-$Eu_2O_3$ solid solution decrease from $a$ = 1.4882 nm, $c$ = 0.3562 nm, $b$ = 0.8960 nm, $\beta$ = 90.26 for the pure $Eu_2O_3$ to $a$ = 1.3086 nm, $c$ = 0.3646 nm, $b$ = 0.8875 nm, $\beta$ = 96.45 for the L20E80 sample at 1500 °C and to $a$ = 1.3505 nm, $c$ = 0.3646 nm, $b$ = 0.8885 nm, $\beta$ = 96.45 for the L20E80 sample at 1600 °C.

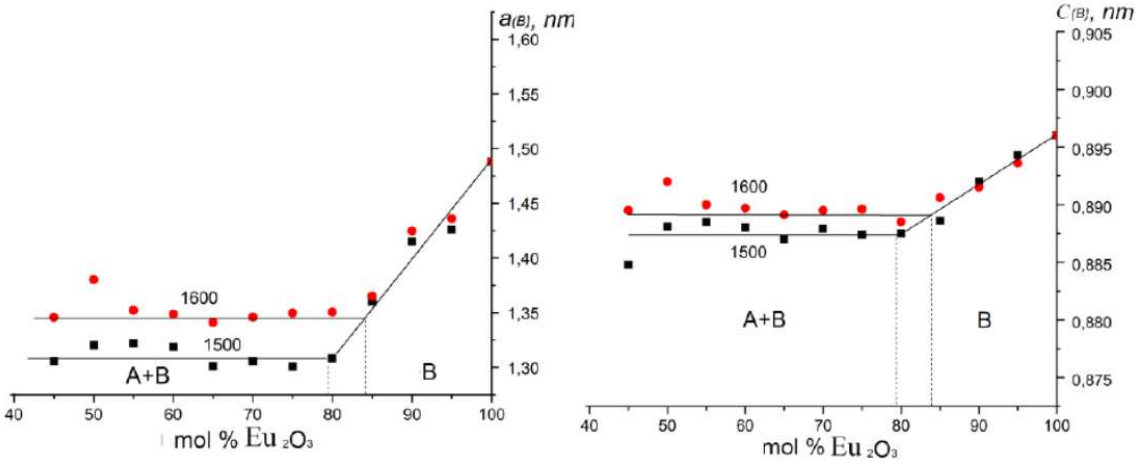


**Figure 3. Concentration dependences of the lattice parameters *a* (a) and *c* (b) of B-$Eu_2O_3$ based solid solutions in the $La_2O_3$-$Eu_2O_3$ system upon annealing at 1500 and 1600 °C**

### 3.2. Phase relation in $CeO_2$-$La_2O_3$-$Eu_2O_3$ system

To study the phase equilibrium in the $CeO_2$-$La_2O_3$-$Eu_2O_3$ system, the following experimental parameters were selected to elucidate location of the four lines: $CeO_2$ - (50 mol% $La_2O_3$ - 50 mol% $Eu_2O_3$), $Eu_2O_3$ - (50 mol% $La_2O_3$ - 50 mol% $CeO_2$), $CeO_2$ - (10 mol% $La_2O_3$ - 90 mol% $Eu_2O_3$) and isoconcentrate 20 mol% $CeO_2$ (Fig. 4). It was established that in the system fields of solid solutions exist based on: hexagonal (A) modification of $La_2O_3$, cubic (F) modification of $CeO_2$ with fluorite-type structure and cubic (C) and monoclinic (B) modifications of $Eu_2O_3$. The systematic study that covered whole composition range excluded formation of new phases. The 1500 °C phase equilibrium in the ternary system $CeO_2$-$La_2O_3$-$Eu_2O_3$ is dominated by those in the constituent binary systems.

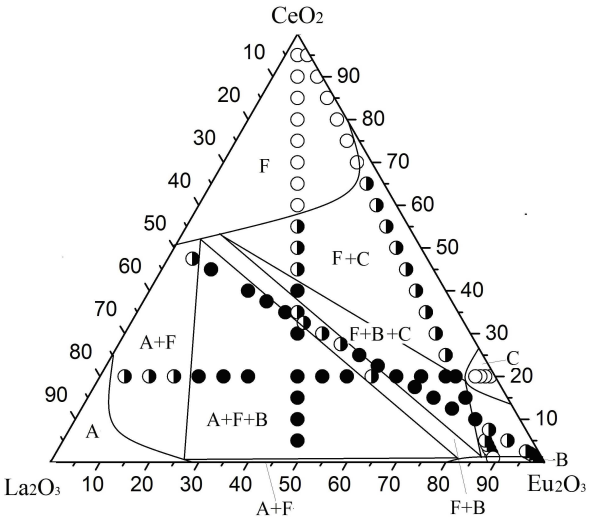


**Figure 4. Isothermal section at 1500 °C for the system $CeO_2$-$La_2O_3$-$Eu_2O_3$ (○ - single-phase samples, ◑ - two-phase samples, ● - three-phase samples)**

Figure 4 depicts the summary of experimental data for the isothermal section of the $CeO_2$-$La_2O_3$-$Eu_2O_3$ system at 1500 °C. The samples were annealed at 1500 °C in air and characterized by X-ray analysis, petrography and scanning electron microscope. The selected XRD patterns that characterize solid solution regions in the $CeO_2$-$La_2O_3$-$Eu_2O_3$ system at 1500 °C are shown in Fig. 5, where the presence of two and three phases is distinctly seen at any percentage of components and phases, which made it possible to carry out an accurate phase analysis. Starting compositions, lattice

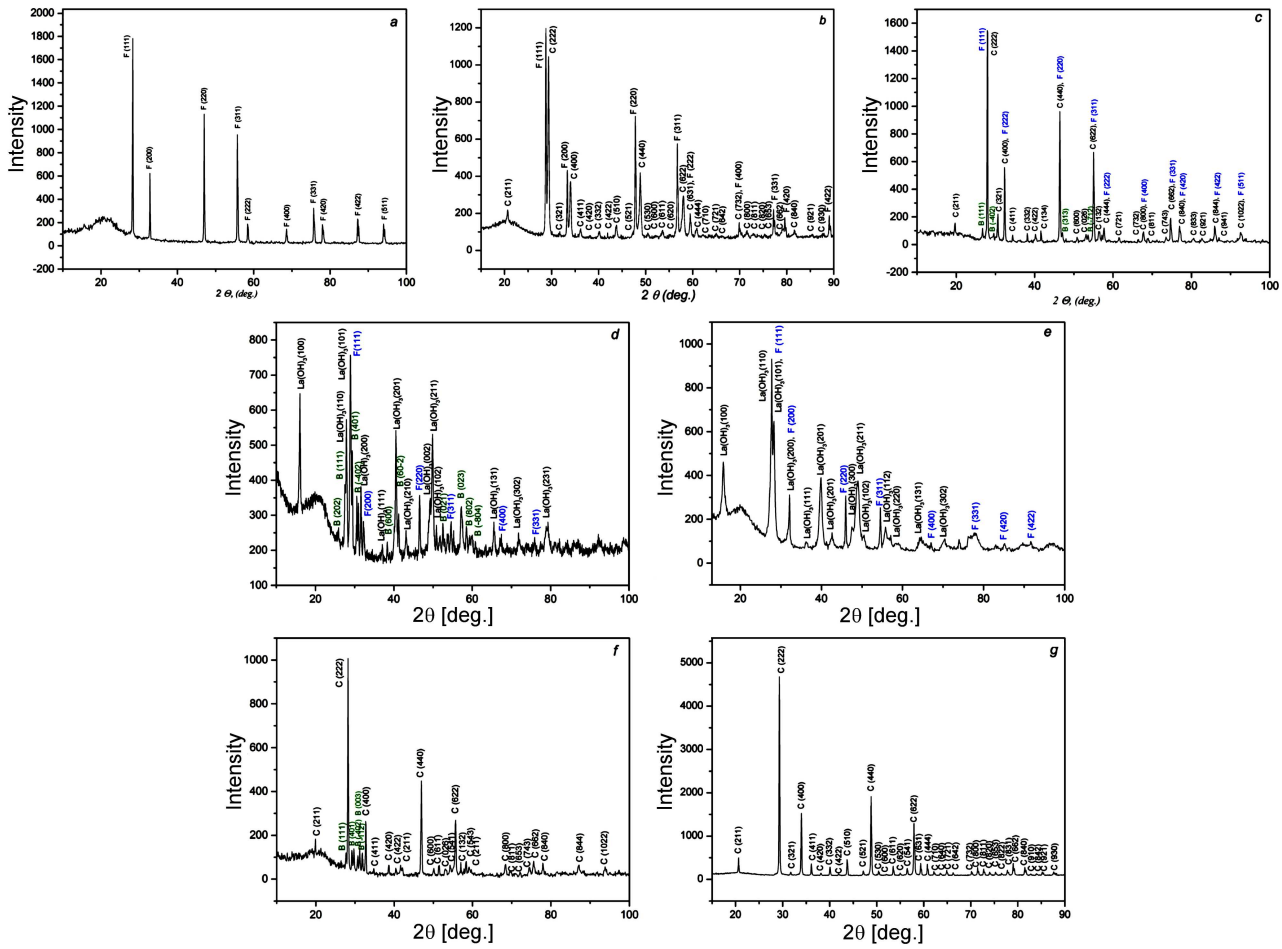


**Figure 5. XRD patterns of the samples from $CeO_2$-$La_2O_3$-$Eu_2O_3$ system annealed at 1500 °C: a) C60-L10-E20 (F), b) C50-L25-E25 (F+C), c) C40-L30-E30 (F+B+C), d) C30-L35-E35 (A+F+B), e) C20-L70-E10 (A+F), f) C1-L1-E98 (B+C) and g) C20-L4-E76 (B+C)**

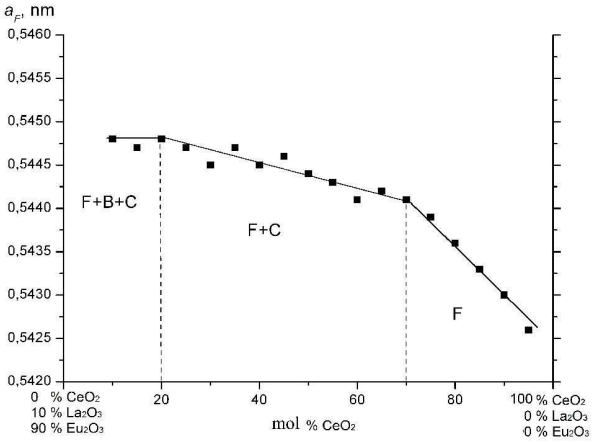


**Figure 6. Concentration dependence of lattice parameters for solid solutions on the basis of F-$CeO_2$ on the section $CeO_2$ - (10 mol% $La_2O_3$ - 90 mol% $Eu_2O_3$) in the $CeO_2$-$La_2O_3$-$Eu_2O_3$ system after annealing of samples at 1500 °C**

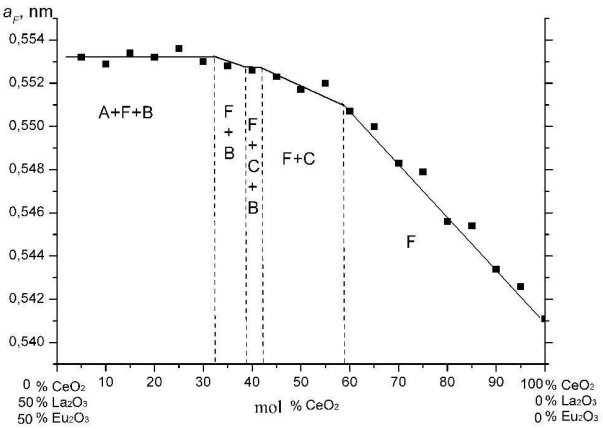


**Figure 7. Concentration dependence of lattice parameters for solid solutions on the basis of F-$CeO_2$ on the section $CeO_2$ - (50 mol% $La_2O_3$ - 50 mol% $Eu_2O_3$) in the $CeO_2$-$La_2O_3$-$Eu_2O_3$ system after annealing of samples at 1500 °C**

parameters and comparison of the identified phases determined by X-ray and petrography techniques are summarized in the Supporting Information (Table 3). The concentration dependences of lattice parameters for F- and C-phases for the binary subsection of $CeO_2$-$La_2O_3$-$Eu_2O_3$ system are presented in Figs. 6-11. The lattice parameters shown in Figs. 6-11 were used to determine the boundaries of the phase fields and the phase compositions.

*F-solid solution*

The cubic ceria-based solid solution has a fluorite-type structure and homogeneity field shows the maximum extension. The boundary of the homogeneity field of F-phase is curved from the center of triangle towards the $CeO_2$ corner and passes through appropriate points in the binary $CeO_2$-$Eu_2O_3$ (80 mol% $CeO_2$) and $CeO_2$-$La_2O_3$ (51 mol% $CeO_2$) systems (Fig. 4). The extent of the F-phase (Fig. 4) is defined by the single-phase compositions (C60-L20-E20 and C70-L3-E27) and two-phase F+C composition (C65-L3.5-E31.5 and C55-L22.5-Eu 22.5).

The lattice parameters also vary from $a$ = 0.5409 nm in the pure $CeO_2$ to $a$ = 0.5442 nm in the two-phase F+C sample C65-L3.5-E31.5 and to $a$ = 0.5448 nm in the three-phase F+B+C sample C20-L8-E72 along the section $CeO_2$ - (10 mol% $La_2O_3$ - 90 mol% $Eu_2O_3$) (Fig. 6). Along the section $CeO_2$ - (50 mol% $La_2O_3$ - 50 mol% $Eu_2O_3$), the lattice parameters vary from $a$ = 0.5409 nm in the pure $CeO_2$ to $a$ = 0.5520 nm in the two-phase F+C sample C55-L22.5-E22.5 and to $a$ = 0.5526 nm in the three-phase F+B+C sample C40-L30-E30 and to $a$ = 0.5528 nm in the two-phase F+B sample C35-L32.5-E32.5 and to $a$ = 0.5530 nm in three-phase A+F+B sample C30-L35-E35 (Fig. 7). Along the section $Eu_2O_3$ - (50 mol% $CeO_2$ - 50 mol%

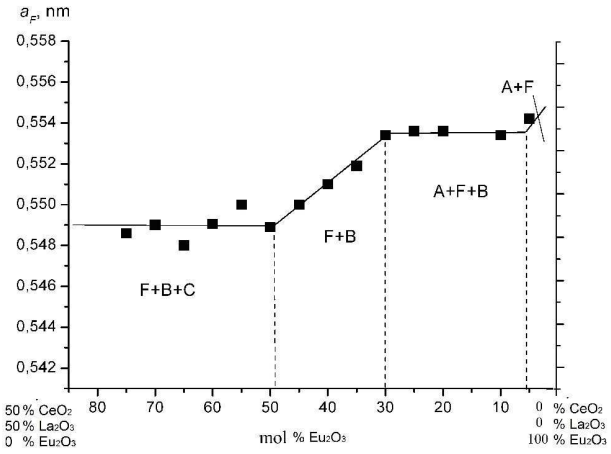


**Figure 8. Concentration dependence of lattice parameters for solid solutions on the basis of F-$CeO_2$ on the section $Eu_2O_3$ - (50 mol% $La_2O_3$ - 50 mol% $CeO_2$) in the $CeO_2La_2O_3$-$Eu_2O_3$ system after annealing of samples at 1500 °C**

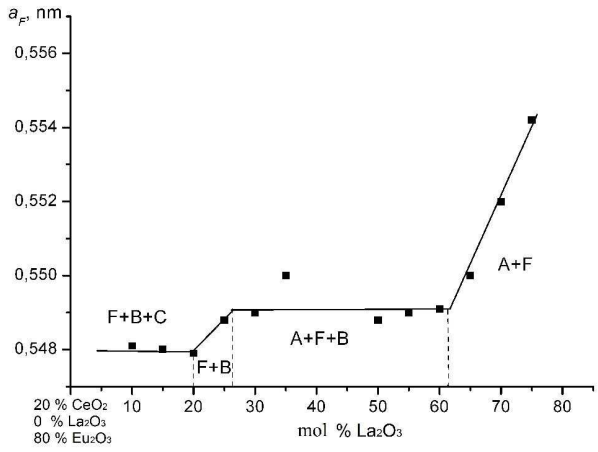


**Figure 9. Concentration dependence of lattice parameters for solid solutions on the basis of F-$CeO_2$ along isoconcentrate 20 mol% $CeO_2$ in the $CeO_2$-$La_2O_3$-$Eu_2O_3$ system after annealing of samples at 1500 °C**

$La_2O_3$) the lattice parameters of F-$CeO_2$ vary from $a$ = 0.5542 nm in the two-phase F+A sample C47.5-L47.5-E5 to $a$ = 0.5534 nm in the three-phase A+F+B sample C45-L45-E10 and to $a$ = 0.5519 nm in the two-phase F+B sample C32.5-L32.5-E35 and to $a$ = 0.5489 nm in the three-phase F+B+C sample C25-L25-E50 (Fig. 8). Finally, along the isoconcetrate 20 mol% $CeO_2$ line changes of the lattice parameter of F-$CeO_2$ faze are shown in Fig. 9.

Dissolution of $Ln^{3+}$ in ceria during annealing in air proceeds by mutual diffusion and solid solution formation through different-valence substitution: $Ln^{3+}$ ions substitute for $Ce^{4+}$ ions in the F-type lattice sites. In order to preserve charge neutrality of the crystal, the difference in ion charge is compensated by the appearance of oxygen vacancies in sites of oxygen ions. There are however such solubility limit values which correspond to a critical concentration of vacancies, beyond which the fluorite-type (*Fm*3*m*) lattice becomes unstable and transforms into another cubic lattice, namely *Ia*3, characteristic for solid solutions of the C-type on the basis of REE oxides.

*B-solid solution*

In the europium-rich corner, the solid solutions based on the monoclinic modification of $Eu_2O_3$ are formed. The phase field B-$Eu_2O_3$ is narrow and elongated (0–19 mol% $CeO_2$) along the $La_2O_3$-$Eu_2O_3$ side of the binary system (Fig. 4). The solubility of $CeO_2$ in the B-$Eu_2O_3$ is low and amounts to ~0.5 mol%, as evidenced by XRD analysis results.

The lattice parameters for B-phase vary from $a$ = 0.1412 nm, $b$ = 0.3609 nm, $c$ = 0.8819 nm, $\beta$ = 99.98 in the two-phase B+C sample C0.5-L0.5-E99 to $a$ = 0.1422 nm, $b$ = 0.3631 nm, $c$ = 0.8879 nm, $\beta$ = 100.47 in the three-phase F+B+C sample C10-L10-E80 and to $a$ = 0.1422 nm, $b$ = 0.3657 nm, $c$ = 0.8950 nm, $\beta$ = 100.16 in the two-phase F+B sample along the section $Eu_2O_3$ - (50 mol% $La_2O_3$ - 50 mol% $CeO_2$) (data are presented in the Supporting Information Table 3). The solid solution based on B-$Eu_2O_3$ is in equilibrium with all phases existing in the ternary $CeO_2$-$La_2O_3$-$Eu_2O_3$ system at 1500 °C.

The difference between B and F solid solutions is in the charge compensation mechanisms. In the fluorite-type solid solutions, the oxygen vacancies compensate the charge difference between $Ce^{4+}$ and $Ln^{3+}$. The fluorite-type lattice allows high concentration of oxygen vacancies and, therefore, the solubility of europia and lanthanum in ceria is high. In opposite, the charge compensation in the ceria substituted $Ln^{3+}$ is defined by the concentration of electrons or oxygen interstitial atoms, which is smaller as compared with concentration of oxygen vacancies in the fluorite-type solid solution.

*C-solid solution*

The phase field C-$Eu_2O_3$ is narrow and elongated (14–26 mol% $CeO_2$) along the $CeO_2$-$Eu_2O_3$ side of the binary system (Fig. 4). The solubility of $La_2O_3$ in the C-$Eu_2O_3$ is up to 6 mol%, along the isoconcentrate 20 mol% $CeO_2$ line (Fig. 4), as evidenced by XRD analysis results.

The lattice parameters for C-phase vary from $a$ = 1.0864 nm in the single-phase sample C20-L1-E79 to $a$ = 1.0907 nm in three-phase C+F+B sample C20-L10-E70 along the isoconcetrate 20 mol% $CeO_2$ line (data are presented in the Supporting Information Table 3). Along the section $CeO_2$ - (10 mol% $La_2O_3$ - 90 mol% $Eu_2O_3$) the lattice parameters for C-phase vary from $a$ = 1.0899 nm in the two-phase C+B sample C2-L9.8-E88.2 to $a$ = 1.0892 nm in the three-phase F+B+C sample C10-L9-E81 and to $a$ = 1.0890 nm in the two-phase F+C sample C25-L7.5-E67.5 (Fig. 10). Along the section $Eu_2O_3$ - (50 mol% $CeO_2$ - 50 mol% $La_2O_3$) the lattice parameters for C-phase vary from $a$ = 1.0835 nm in the two-phase B+C sample C0.5-L0.5-E99 to $a$ =

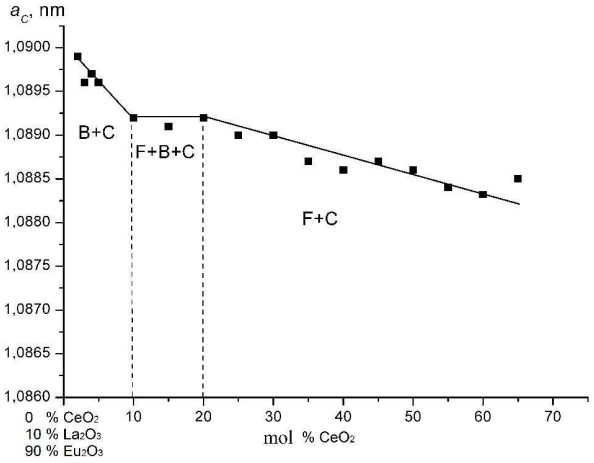


**Figure 10. Concentration dependence of lattice parameters for solid solutions on the basis of C-$Eu_2O_3$ on the section $CeO_2$ - (10 mol% $La_2O_3$ - 90 mol% $Eu_2O_3$) in the $CeO_2$-$La_2O_3$-$Eu_2O_3$ system after annealing of samples at 1500 °C**

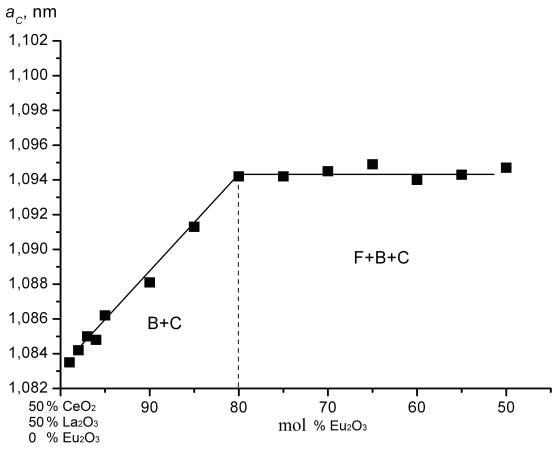


**Figure 11. Concentration dependence of lattice parameters for solid solutions on the basis of C-$Eu_2O_3$ on the section $Eu_2O_3$ - (50 mol% $La_2O_3$ - 50 mol% $CeO_2$) in the $CeO_2$-$La_2O_3$-$Eu_2O_3$ system after annealing of samples at 1500 °C**

1.0942 nm in the three-phase F+B+C sample C10-L10-E80 (Fig. 11).

*A-solid solution*

The homogeneity field of solid solution based on A-$La_2O_3$ extends to 25 mol% $CeO_2$ and 28 mol% $Eu_2O_3$ in the corresponding binary systems (Fig. 4). It should be noted that the samples with higher lanthanum oxide content after annealing and cooling rapidly absorb water in humid air and become hydrated. Hence, according to XRD, the hexagonal A-$La(OH)_3$ modification is formed instead of the hexagonal A-$La_2O_3$ phase.

## IV. Conclusions

The phase equilibria in the $La_2O_3$-$Eu_2O_3$ system were studied at 1500 and 1600 °C in the whole concentration range using XRD. The system was characterized by formation of solid solutions with a hexagonal (A-$La_2O_3$) and monoclinic (B-$Eu_2O_3$) structures separated with a wide heterogeneous region A+B. Homogeneous boundary regions of A-$La_2O_3$ based solid solutions correspond to the following compositions: 100–72 mol% $La_2O_3$ at 1500 °C, 100–62 mol% $La_2O_3$ at 1600 °C. As temperature reduces from 1600 to 1500 °C, the homogeneity regions of solid solutions based on the monoclinic modification B-$Eu_2O_3$ narrow from 84 to 81 mol% $La_2O_3$. In accordance with Vegard's law the lattice parameter linearly decreases. The 1500 °C phase equilibria in the ternary $CeO_2$-$La_2O_3$-$Eu_2O_3$ system were studied for the first time over the entire triangle composition, and the 1500 °C section of the $CeO_2$-$La_2O_3$-$Eu_2O_3$ phase diagram was constructed. The solid solutions of limited solubility based on all components in their different polymorphic modifications were found and characterized. The ceria-based fluorite solid solutions are represented by the largest homogeneity field originating from the sizes of F-fields in the two boundary binary systems $CeO_2$-$La_2O_3$ and $CeO_2$-$Eu_2O_3$. It was revealed that in the $CeO_2$-$La_2O_3$-$Eu_2O_3$ system the phases of cubic symmetry predominate such as: F - *Fm*3*m*, C - *Ia*3. The isothermal section of the $CeO_2$-$La_2O_3$-$Eu_2O_3$ system at 1500 °C contains two three-phase regions (A+F+B, F+B+C) and five two-phase regions (F+A, A+B, B+F, F+C, C+B).

§ Supporting Information can be downloaded using following link: https://bit.ly/3diC9r7

## References


1. B. Wang, B. Zhu, S. Yun, W. Zhang, C. Xia, M. Afza, Y. Cai, Y. Liu, Y. Wang, H. Wang, "Fast ionic conduction in semiconductor $CeO_{2-\delta}$ electrolyte fuel cells", *NPG Asia Mater.*, **51** (2019) 1–12.
2. C.X. Hua, "Lithium storage mechanism and catalytic behavior of $CeO_2$", *Electrochem. Commun.*, **25** (2012) 66–69.
3. T. Hong, Y.X. Zhang, K. Brinkman, "Enhanced oxygen electrocatalysis in heterostructured ceria electrolytes for intermediate-temperature solid oxide fuel cells", *ACS Omega*, **3** (2018) 13559–13566.
4. L. Ping, Ch. Xiaoyin, L. Yongdan, S.W. Johannes, "A review on oxygen storage capacity of $CeO_2$-based materials: Influence factors, measurement techniques, and applications in reactions related to catalytic automotive emissions control", *Catal. Today*, **327** (2018) 90–115.
5. E.R. Andrievskaya, O.A. Kornienko, O.I. Bykov, A.V. Sameljuk, Z.D. Bohatyriova, "Interaction of ceria and ytterbia in air within temperature range 1500–600 °C", *J. Eur. Ceram. Soc.*, **39** (2019) 2930–2935.
6. O.A. Kornienko, A.V. Sameljuk, O.I. Bykov, Yu.V. Yurchenko, A.K. Barshchevskaya, "Phase relation studies in the $CeO_2$-$La_2O_3$-$Er_2O_3$ system at 1500 °C", *J. Eur. Ceram. Soc.*, **40** (2020) 4184–4190.
7. J. Gulicovski, S. Nenadović, L. Kljajević, M. Mirković, M. Nišavić, M. Kragović, M. Stojmenović, "Geopolymer/$CeO_2$ as Solid Electrolyte for IT-SOFC", *Polymers*, **248** (2020) 2–19.
8. S.I. Ahmad, "Nanostructured cerium oxide (ceria): electrolyte for IT-SOFC", *Int. J. Nano Res.*, **1** (2018) 11–13.
9. S. Li, X. Lu, S. Shi, L. Chen, Z. Wang, Y. Zhao, "Europium-doped ceria nanowires as anode for solid oxide fuel cells", *Frontiers Chem.*, **8** (2020) 1–10.
10. O. Kornienko, O. Bykov, A. Sameliuk, Y. Yurchenko, "Phase relation studies in the $CeO_2$-$La_2O_3$-$Eu_2O_3$ system at 1250 °C", *Ukrainian Chem. J.*, **86**, (2020) 37–45.
11. B.P. Mandal, V. Grover, A.K. Tyagi, "Phase relations, lattice thermal expansions in $Ce_{1-x}Sm_xO_{2-x/2}$ systems and stabilization of cubic $RE_2O_3$ (RE: Eu, Sm)", *Mater. Sci. Eng. A*, **430** (2006) 120–124.
12. V. Grover, A. Banerji, P. Sengupt, A.K. Tyagi, "Raman, XRD and microscopic investigations on $CeO_2$-$Lu_2O_3$ and $CeO_2$-$Sc_2O_3$ systems: A sub-solidus phase evolution study", *J. Solid State Chem.*, **181** (2008) 1930–1935.
13. O.R. Andrievskaya, O.A. Kornienko, O.I. Bykov, A.V. Sameliuk, Z.D. Bohatyriova, "Interaction of ceria and erbia in air within temperature range 1500–600 °C", *J. Eur. Ceram. Soc.*, **40** (2020) 3098–3103.
14. M. Stopyra, I. Saenko, M. Ilatovskaia, G. Savinykh, O. Fabrichnaya, "Phase relations in the $ZrO_2$-$La_2O_3$-$Gd_2O_3$ system: experimental studies and phase modeling", *J. Am. Ceram. Soc.*, **102** (2019) 7628–7644.
15. E.R. Andrievskaya, O.A. Korniienko, A.I. Bykov, A.V. Sameljuk, "Phase relation studies in the $ZrO_2$-$La_2O_3$-$Gd_2O_3$ system at 1600 °C", *Pow. Metall. Met. Ceram.*, **58** (2020) 714–724.
16. M. Ilatovskaia, S. Sun, I. Saenko, G. Savinykh, O. Fabrichnaya, "Experimental investigation of phase relations in the $ZrO_2$-$La_2O_3$-$Yb_2O_3$ system", *J. Phase Equilib. Diffus.*, **41** (2020) 311–328.
17. J.P. Traverse, *Contribution au developpement de méthodes d'experimentation a temperature elevée: application a l'étude du polymorphisme des sesquioxydes de terres rares et des changements de phases dans les systems zirconechaux et zircone-oxyde de strontium*, Thése L'Univérsite Scientifique et Medicale de Grenoble, Grenoble, 1971.
18. H. Yamamura, H. Nishino, k. Kakinuma, "AC conductivity for $Eu_2Zr_2O_7$ and $La_2Ce_2O_7$ with pyrochlore-type composition", *J. Ceram. Soc. Jpn.*, **111** (2003) 907–911.
19. S.A. Toropov, *Phase Diagrams of the Refractory Oxide Systems, Binary Systems*, Chapter 3, Leningrad, Nauka, 1987.

20. B.A. Kumar, V. Sankaranarayanan, "Ionic transport properties in nanocrystalline $Ce_{0.8}A_{0.2}O_{2-\delta}$ (with A = Eu, Gd, Dy, and Ho) materials", *Nanoscale Res. Lett.*, **5** (2010) 637–643.
21. N.M. Masaki, A. Nakamura, F. Furuuchi, Y. Hinatsu, "$^{151}$Eu-Mössbauer spectroscopic and X-ray diffraction study of the $Eu_2(Ce_{1-x}Zr_x)_2O_7$ and $LnEuZr_2O_7$ (Ln = lanthanide) systems", *J. Phys. Chem. Solids*, **66** (2005) 312–317.
22. E.R. Andrievska, O.A. Kornienko, A.V. Sameliuk, A. Sair, "Phase relation studies in the $CeO_2$-$Eu_2O_3$ system at 1500 to 600 °C in air", *J. Eur. Ceram. Soc.*, **40** (2020) 751–758.
23. E.R. Andrievskaya, O.A. Kornienko, A.V. Sameljuk, A. Sayir, "Phase relation studies in the $CeO_2$-$La_2O_3$ system at 1100–1500 °C", *J. Eur. Ceram. Soc.*, **31** (2011) 1277–1283.
24. E.R. Andrievskaya, O.A. Kornienko, A. Sayir, O.O. Vasylkiv, S. Yoshio, "Phase relation studies in the $ZrO_2$-$CeO_2$-$La_2O_3$ system at 1500 °C", *J. Am. Ceram. Soc.*, *94* (2011) 1911–1919.
25. B.C. Morris, W.R. Flavell, W.C. Mackrodt, M.A. Morris, "Lattice parameter changes in the mixed oxide system $La_xCe_{1-x}O_{2-x/2}$ - A combined experimental and theoretical study", *J. Mater. Chem.*, **3** [10] (1993) 1007–1013.
26. F. Sibieude, G. Schiffmacher, P. Caro, "Étude au microscope électronique de structures modulées dans les régions systéme $La_2O_3$-$CeO_2$ riches en $La_2O_3$", *J. Solid State Chem.*, **23** (1968) 361–367.
27. N. Minkova, S. Aslanian, "Isomorphic substitutions in the $CeO_2$-$La_2O_3$ system at 850 °C", *Cryst. Res. Technol.*, **24** (1984) 351–354.
28. E.R. Andrievskaya, *Phase Equilibria in the Systems of Hafnia, Yttria with Rare-Earth Oxides*, Scientific book Project, Kiev, Naukova Dumka, 2010, 470 p.